J Syst Sci Complex (2013) 26: 695–717

PLANNING OF DYNAMICALLY FEASIBLE TRAJECTORIES FOR TRANSLATIONAL, PLANAR, AND UNDERCONSTRAINED CABLE-DRIVEN ROBOTS*

TREVISANI Alberto

DOI: 10.1007/s11424-013-3175-1
Received: 22 January 2013 / Revised: 19 February 2013

Abstract Extensively studied since the early nineties, cable-driven robots have attracted the growing interest of the industrial and scientific community due to their desirable and peculiar attributes. In particular, underconstrained and planar cable robots can find application in several fields, and specifically, in the packaging industry. The planning of dynamically feasible trajectories (i.e., trajectories along which cable slackness and excessive tensions are avoided) is particularly challenging when dealing with such a topology of cable robots, which rely on gravity to maintain their cables in tension. This paper, after stressing the current relevance of cable robots, presents an extension and a generalization of a model-based method developed to translate typical cable tension bilateral bounds into intuitive limits on the velocity and acceleration of the robot end effector along a prescribed path. Such a new formulation of the method is based on a parametric expression of cable tensions. The computed kinematic limits can then be incorporated into any trajectory planning algorithm. The method is developed with reference to a hybrid multi-body cable robot topology which can be functionally advantageous but worsen the problem of keeping feasible tensions in the cables both in static and dynamic conditions. The definition of statically feasible workspace is also introduced to identify the positions where static equilibrium can be maintained with feasible tensions. Finally, some aspects related to the practical implementation of the method are discussed.

Keywords Cable robot, dynamically feasible trajectories, statically feasible workspace, trajectory planning.

TREVISANI Alberto
Department of Management and Engineering (DTG), Università degli Studi di Padova, Stradella S. Nicola 3, 36100 *Vicenza, Italy.* Email: alberto.trevisani@unipd.it.
*This research was supported by the Università degli Studi di Padova under Grant No. CPDA088355/08.
◇ *This paper was recommended for publication by Guest Editor LI Hongbo.*

1 Introduction and State of the Art

1.1 Cable Robots: Advantages and Applications

Cable-driven robots, or simply cable robots, are relatively simple robotic manipulators formed by attaching multiple cables to an end effector. In cable robots the cables are usually active, in the sense that they are driven by motors that can extend or retract the cables by winding or unwinding them from pulleys or winches. Cable robots have several desirable advantages over conventional robots, which have been recognized since the early studies in the field[1, 2]. Primarily, they can be designed to have a very large workspace (because the winches may unwind a large amount of cable), a very high load capacity (comparable to that of construction cranes), or to generate very high speed motions (because of their low inertial properties). Additionally, their simple design makes them relatively inexpensive, modular, transportable, and easily reconfigurable. Finally, their minimal moving mass makes them very energy efficient, and their low invasiveness makes them good candidates for interaction with human operators, for example in medical robotics. All these advantages are promoting the deployment of cable robots in several real-world applications such as:

1) heavy payload handling[1, 3], including unloading cargo from a ship[4] and load transportation[5];
2) high speed manipulation[6, 7];
3) aircraft maintenance and large-scale inspection[8, 9];
4) positioning and measuring systems in wind tunnels[10];
5) haptics[11–13];
6) metrology[9, 14];
7) surgery[15];
8) rehabilitation[16, 17];
9) large scale radio telescopes[18];
10) sport and entertainment[19, 20];
11) rescue and emergency services[21, 22];
12) building painting and servicing[23].

The aforementioned applications, which represent just a partial list, are not simply prospective applications: lots of these ideas have been put into practice through working prototypes. In particular, a number of cable robot families has been successfully developed to date:

- The RoboCrane developed by the American National Institute of Standards and Technology (NIST)[1]. Such a cable robot family was probably the first to be presented, in the early 90's, and was subsequently applied to numerous applications including, but not limited to, heavy or light material handling, macro and micro machining through dual manipulators, airplane inspection and repair, and field inspection.

- The IPAnema by the Fraunhofer IPA in Germany[9]. The major goal in the development of this family of cable robots has been using only industrial grade components which, on the one hand, can assure a considerable reliability and robustness in industrial applications,

but, on the other hand, pose large restrictions to the complexity of the algorithms adopted to operate a robot. This family of robots is being designed to operate within a very large working area, at high speeds and extreme accelerations, and with a very wide payload range. Several applications, ranging from airplane maintenance to building of enormous solar-thermal plants, have been predicted for this cable robot family.

- The Marionet designed in France at the INRIA[22]. This family of cable robots includes small size prototypes for high speed applications, but it is better known for a portable crane for rescue, and components for home assistance of people with disability.

The appropriateness of cable robots to medical and welfare use has been widely recognized and has led to some other very interesting prototypes, mainly in the rehabilitation field: one family of rehabilitation robots for post-stroke patients has been developed in Italy and includes the NeReBot and the MariBot[16]. In particular, the MariBot, is basically a hybrid robot with an active SCARA-like serial support and a cable suspended end effector. A completely different design of cable robot for rehabilitation, which operates as an exoskeleton, has been instead proposed in [17] and named CAREX.

A very challenging concept and design of cable robot which is also worth mentioning and which is expected to be operative by 2016, is the light-weight feed cabin of the Chinese Five-hundred-meter Aperture Spherical radio Telescope (FAST)[18]. The FAST will be built in a natural karst depression and is designed to become the most sensitive single dish radio telescope ever built. From the engineering viewpoint the design of the cable-driven feed cabin of the FAST is extremely demanding since the huge size of the telescope does not allow relying on some typical assumptions made when studying cable robots, such as that cables are massless and perfectly stiff. Hence, modeling, trajectory planning, and motion control become much more complicate.

1.2 Cable Robot Topologies

Different cable robot topologies have been proposed to date. The alternative topologies lead to possible classifications of cable robots. So far, there is no single classification universally recognized, not even the terminology adopted is unified.

Generally speaking, cable robots can be either planar or spatial. In other words, cable robots may operate in planar or spatial arrangements. In the first case (see, e.g., [24]) the end effector is forced to move within a plane of motion, while in spatial cable robots (see, e.g., [25]) the end effector can move in a three dimensional workspace.

Planar and spatial cable robots are said to be translational (see, e.g., [26]) when no rotational degrees of freedom (dofs) can be given to the end effector because, for example, all the cables converge in a single point (see, e.g., [27]).

Cable robots are usually said to be fully actuated (see, e.g., [28]) if they have a number of actuating cables, and hence of motors, equal to the number of dofs of the end effector. Conversely, redundant (or redundantly actuated) robots (see, e.g., [29]) have a number of active cables which is greater than the number of dofs of the end effector. A cable robot can also be

underactuated if the number of degrees of freedom of the end effector is greater than the number of active cables. Indeed, a cable robot can also become underactuated if some active cables become slack during the motion. The computation of the pose of the end effector starting from the lengths of the cables or, in other words, the solution of the forward kinematics problem for underactuated cable robots is not trivial, and may lead to several real solutions in spatial arrangements. Additionally, the solutions depend on the forces applied, which complicates the analysis considerably[30].

When focusing on the restraining capability of the cables, it is possible to distinguish between underconstrained and fully constrained cable robots. Generally speaking, a cable robot is fully constrained if, assuming unbounded cable tensions, it can maintain equilibrium against all external wrenches. The advantage of fully constrained configurations is apparent: while an underconstrained cable robot must rely on gravity to keep positive tensions in the cables, fully constrained cable robots can take advantage of the redundant cable to set a desired tension distribution in the cables[31]. As a matter of fact, in order to fully constrain the end effector of a cable robot, it is required that the number of cables is greater by one than the number of dofs of the end effector (see, e.g., [13]). A higher number of cables may also lead to overconstrained configurations (see, e.g., [32]). It is important to underline that the aforementioned conditions on the number of cables are only necessary but not sufficient: in some cable arrangements a cable robot can be underconstrained even if the number of cables is greater than the number of dofs; in other words, a cable robot can concurrently be redundant and underconstrained (see, e.g., [33]). Clearly, when the number of cables is less than or equal to the number of dofs (see, e.g., [34]), the robot is necessarily underconstrained (sometimes also called cable-suspended), and hence, there exists a wrench against which equilibrium is not maintained.

Finally, cable robots can be classified as single-body and multi-body cable robots[35]. In all the references quoted so far, the cable robots considered are single-body ones, i.e., all the cables are attached to a rigid-body end effector. Conversely, in multi-body cable robots the cables are attached to different links of a multi-body, typically a serial manipulator (see, e.g., [36, 37]).

1.3 Cable Robot Chief Weaknesses

As previously underlined, cable robots have some very desirable advantages, however they also experience certain limitations which can be more or less severe based on the topology.

Firstly, in all cable robots an important additional constraint applies to motion planning and control: cables can pull but are unable to push the end effector, which obliges to keep the forces in all cables positive during normal operation. Additionally, not only cables should be prevented from becoming slack, but excessive cable tensions should be also avoided during motion.

Another limitation derives from the fact that usually, the end effector position cannot be measured directly. Inaccuracies at the end effector can therefore result from cable stretching and sagging, variation in cable spool properties (e.g., spool diameter increases with the number of windings if no dedicated design is adopted[9]), and calibration issues.

A further disadvantage is the limited force application in some configurations and directions

(e.g., in underconstrained robots the downward force capabilities depend on the gravity force and hence are limited to the payload weight).

Additionally, the coordination of redundant cables, and the avoidance of cable interference may require complex control schemes and more sensors. Cable interference can also limit the orientation capacity of the robot end effector, and generally speaking can limit the robot workspace.

Finally, the worksite where a cable robot is to be installed needs to be suitably prepared: not only there must not be obstacles which can be hit by the cables, but the structures to which motors, winches, and guiding pulleys are fitted must be suitably designed, since cable tensions can become extremely high (in particular in heavy payload handling), and it can be very dangerous to fix a cable robot on structures that were not meant for that use[38].

1.4 A Hybrid Multi-Body Cable Robot Topology for High-Speed Manipulation

Further research efforts and design refinements are needed to overcome the aforementioned limitations, however, in consequence of their advantages cable robots are likely to find successful application in industrial and service robotics, and promise to significantly increase performances in terms of payload, workspace and dynamics[9]. In particular, with reference to the improvement of the dynamic performances, it is known that it is an ever increasing requirement for augmenting the throughput and the efficiency of production systems. This is particularly true in the fast moving consumer goods (FMCG) industry, and in particular in the packaging industry, where a very successful effort has been made to increase robot speed to make it suitable for in-process operations (such as picking, collating, and sorting) where traditional serial robots cannot be employed because they do not have adequate speed. Planar robots are extensively employed in these operations. With either serial or parallel topology, they are typically used to manipulate parts over the belt. There end effectors possess a minimum of two translational dofs. An additional rotational dof is given in case object orientation must be changed. A great effort has been devoted to try to keep moving inertia to a minimum in these robots by employing very light-weight materials and mounting the heaviest motors on the frame.

It is apparent that cable-driven robots have a great potential in this field since they benefit from minimal moving inertia. Of course, if a planar cable robot has to be designed for high-speed manipulation, it is of paramount importance that it is adequately stiff against loading normal to the motion plane. In cable robots stiffness is usually achieved through redundant actuation. However, redundant actuation has some major limitations: first of all it is expensive, additionally cables tend to obstruct the workspace, and sometimes cable interference can be difficult to avoid.

The hybrid and underconstrained design initially proposed in [39] (and derived from the one introduced in [40] for a redundant translational planar cable robot) can overcome these limitations while exploiting the advantages of cable actuation. The proposed design could be thought of as a merger of a serial and parallel planar manipulator, both moving in the vertical plane, where, however, the rigid links of the parallel manipulator are replaced by two active cables. As a matter of fact, as shown in the scheme in Figure 1 (on the left), the robot consists

of two actuated winches mounted on a fixed frame which are used to control the extension of two coplanar active cables. The cable output (or "attachment") points are fixed and coincide with the vertices A_1 and A_2 at the top of the rectangular base polygon which is plotted in gray and whose side lengths are L_A and L_B. The two cables, whose angles are θ_1 and θ_2, drive the end effector which is modeled as a point mass located at the free end of a two-dof serial linkage. The serial linkage is passive in the sense that both the revolute joints of the serial linkage are passive. Contrary to a few hybrid multi-body cable robots already appeared in [35–37], in this robot the two coplanar active cables drive directly the end effector rather than the links of the serial manipulator, which basically supports the end effector to reduce out-of-plane compliance. The robot has therefore two cables, driven by two actuated winches, providing two translational motions to the end effector in the vertical plane. Hence, the robot is fully actuated and non redundant: it does not have more cables than necessary to control the two translational degrees of freedom of the end effector, which are the two Cartesian coordinates of its tool center point (TCP). The TCP is assumed coinciding with the point where cables converge.

This hybrid multi-body topology has some desirable advantages that can be summarized as follows:

- a reduced out-of-plane compliance thanks to the serial linkage,
- a minimum use of actuators making the robot relatively inexpensive,
- a limited cable obstruction in the workspace and a completely free workspace below the end effector thanks to the non redundant design,
- a high payload-to-weight ratio (the components of the serial linkage can be lightweight because the links do not have to sustain dynamic loading),
- improved accuracy in the measurement of the end effector position, since the serial linkage can also serve as an independent metrology system when adding encoders to its passive joints. This prevents measuring errors due to cable elasticity,
- moment resistance at the end effector is provided by the serial linkage.

These features are likely to make such a hybrid multi-body design suitable not only for industrial use, but also for medical and welfare use, in particular for rehabilitation.

A prototype of such a robot has been presented in [41] (see Figure 1, on the right), to which the interested reader is referred for the details on the robot geometrical and inertial features. Here only some basic information is provided: the robot cables are made of Dyneema® and are driven by brushless servomotors, the links of the serial linkage are made of aluminum and, just to convey the idea of the size of the robot prototype, $L_A = 1.108$m, $L_B = 0.712$m, and the lengths of the two links are identical and equal to 0.622m.

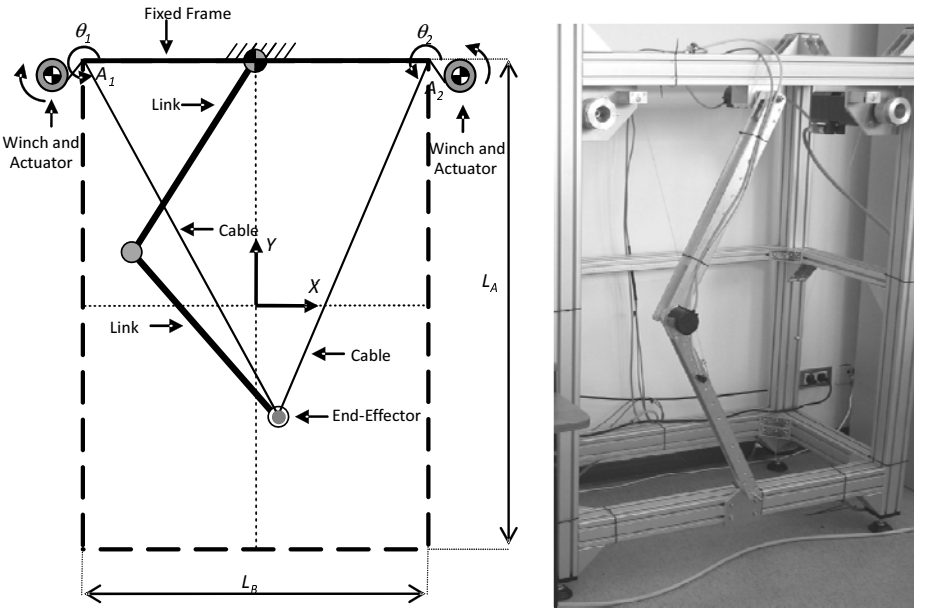

Figure 1 Scheme of the hybrid cable robot (on the left) and picture of a laboratory prototype (on the right)

2 Motivation and Objectives

A major requirement that has to be met in cable robots is ensuring that during operation all cables are under tension, and that such a tension is below the maximum permissible value related to the torque limits of the actuators or to the tensile force limits of the cables.

There is a large body of work addressing the issue of maintaining positive tensions in cables (see, e.g., [29, 40, 42]), including the work in [43] which focused on a time-optimal trajectory planning strategy capable of assuring that cable forces can be maintained tensile along a prescribed paths. In general, in fully constrained and overconstrained cable robots it is possible to rely on redundant cables to guarantee positive cable tensions, but this opportunity raises another issue: at any point in a trajectory there exists an infinity of possible sets of cable tensions and one generally needs a computationally efficient algorithm capable to find a feasible set, possibly satisfying some optimality criterion and guaranteeing the continuity of cable tensions along a given trajectory[31].

As previously mentioned, assuring feasible tensions in all cables along a trajectory (a trajectory is feasible if the tensions in all cables are not only positive, but also bounded) is particularly difficult in underconstrained robots, where redundancy cannot been exploited (as for example in [40]). In the hybrid multi-body topology presented above, such a problem is exacerbated by

the presence of the serial linkage, which considerably affects the robot workspace and dynamics. As a matter of fact, the serial linkage produces a reaction force acting on the end effector which is neither constant in amplitude nor in direction. As a consequence, such a force does not necessarily increase the tensions in the cables, as gravity usually does, but it can have either beneficial or detrimental effects on tensions depending on the configuration and the prescribed motion of the cable robot. These effects must be accounted for both during motion and at rest. Indeed, to be feasible, a rest-to-rest trajectory also imposes that static equilibrium can be maintained at the start point and the end point. Therefore studying the features of the workspace is an essential preliminary activity which is also addressed in this paper.

A successful approach to prevent cable slackness and excessive tensions in underconstrained cable robots may consist in making use of the dynamic model of a cable robot to translate cable tension bilateral bounds (i.e., positive and bounded tensile cable forces) into bounds on the velocity and acceleration of the robot end effector along an assigned path. Such kinematic limits can then be incorporated into any trajectory planning algorithm. This approach has been introduced in [39] and experimentally validated in [41] by applying it to the hybrid multi-body robot presented above, which is used as a representative example of translational, planar and underconstrained cable robot for which, as previously mentioned, the planning of dynamically feasible trajectories is particularly challenging. In both [39] and [41] the formulation has been restricted to two paths of industrial interest: the straight line and the circular paths. Here a more general formulation is inferred which is valid for any path and relies on a parametric formulation of the cable tensions along a generic path. In particular, the method allows defining a criterion to set a limit to the maximum velocity achievable by the end effector TCP along the path and allows computing positive upper bounds and negative lower bounds for the acceleration of the end effector TCP. As long as these kinematic limits are satisfied it is proved that proper cable tensioning is assured.

Hence, the method proposed is not a so-called trajectory verifier, i.e., an algorithm determining whether a defined trajectory can be reached, but a method to a-priori satisfy cable tension constraints. Indeed, in a real robot the actual tensions can match the theoretical ones only if an effective motion controller is available (as for example the centralized one proposed in [40]). The controller must ensure limited tracking error, which is however a conventional specification in robotics.

Another advantage of the method is its low computational complexity which makes it suitable for implementation in real time systems. This feature is of paramount importance for prospective industrial use.

The organization of the paper is as follows. In Section 3, the definition of statically feasible workspace (SFW) is introduced and applied to the hybrid multi-body cable robot here employed as an example of generic translational planar and underconstrained cable robot. In Section 4, the expression of the cable tensions during motion is developed in parametric form (i.e., as a function of the scalar path parameter). The kinematic limits ensuring positive and bounded cable tensions for any path through space are then computed in Section 5. Aspects related to the practical application of the theory developed are discussed in Section 6. Concluding

remarks are finally given in Section 7.

3 The Statically Feasible Workspace (SFW)

3.1 Workspace Definitions

In cable robotics literature, several definitions of workspace have been proposed and the terminology is far from being unified. In this section only the most popular definitions are recalled before introducing the new definition of Statically Feasible Workspace (SFW).

The static equilibrium workspace (SEW)[27] or simply static workspace[44] is defined as the set of end effector poses for which static equilibrium can be obtained while maintaining tension in all cables. This definition assumes infinite maximum cable lengths and tensions, additionally only the effect of gravity is usually considered. By including in the SEW definition the effect of external wrenches (i.e., forces and torques applied to the end effector) one gets the definition of wrench-closure workspace (WCW)[45], which is the set of poses for which any wrench can be generated at the end effector while maintaining tension in all cables. Sometimes the WCW is also called controllable workspace[35]. In the WCW definition both cable tensions and wrench sets are unbounded, if one considers the more practical case in which both cable tensions and wrench sets are bounded, it is possible to get the definition of wrench-feasible workspace (WFW)[46] as the set of end effector poses in which a specified range of external wrenches can be generated using a limited range of cable tensions. The force-closure workspace (FCW)[47] is instead a special case of WFW whose required set of wrenches is the whole set of wrenches and the only constraint on the cable tensions is non-negativity. Another workspace definition which does not have an equivalent in traditional serial robotics is the dynamic workspace[44] which is defined as the set of end effector configurations for which a specific dynamic equilibrium is possible, or, in other words as the set of poses that the end effector can reach with at least one kinematic state (position, velocity, and acceleration)[48].

To the author's best knowledge, in literature there lacks a suitable definition of workspace in the case static equilibrium is considered, no external wrenches are applied to the end effector, and both the positivity and boundedness constraints on cable tensions are imposed. It is therefore useful to introduce the statically feasible workspace (SFW), defined as the set of end effector poses for which static equilibrium against gravity can be obtained using a limited range of cable tensions. Clearly, the SFW may be thought of as a special case of WFW when just the gravity wrench is considered: in the SFW static equilibrium can be maintained against gravity with positive and bounded cable tensions. It is recognized that the term "statically feasible workspace" was first applied to cable robots in [49] where, however, no formal definition was provided.

3.2 Computation of the SFW for the Studied Cable Robot

Now, refer to the free body diagram of the end effector shown in Figure 2, where the end effector is modelled as a point mass. Henceforth it will be assumed that Coulomb friction can be neglected, that all the links are rigid and that all the cables are massless and perfectly stiff.

Additionally, boldfaced lower-case letters will be used to represent vectors while boldfaced upper-case letters will be reserved for matrices. The scalars and the entries of vectors and matrices will instead be denoted with lowercase italic letters.

The static equilibrium equation for the end effector takes the form:

$$\boldsymbol{p_E} + \boldsymbol{p_S} + \boldsymbol{f_T} = \boldsymbol{0}, \tag{1}$$

where:

- vector $\boldsymbol{p_E}$ is the weight force vector applied to the end effector. Within the whole workspace it takes the constant form $\boldsymbol{p_E} = \{\ 0 \quad -Mg\ \}^{\mathrm{T}}$, with M the overall mass of the end effector, also including the pay-load.
- vector $\boldsymbol{p_S}$ is the static component (i.e., the gravitational one) of the force exerted by the passive serial linkage on the end effector. It can be computed through the equilibrium equations of the serial manipulator links[39]. Both the magnitude and the direction of $\boldsymbol{p_S}$ vary within the workspace.
- vector $\boldsymbol{f_T}$ is the resultant force exerted by cable tensions on the end effector. If we denote by $\boldsymbol{\tau}$ the vector of the cable tensions, this simple relation holds between $\boldsymbol{f_T}$ and $\boldsymbol{\tau}$: $\boldsymbol{f_T} = \boldsymbol{S\tau}$, where $\boldsymbol{S}$ is the pseudostatics Jacobian, whose elements are trigonometric functions of the cable angles θ_1 and θ_2[40]. Since the robot is underconstrained, $\boldsymbol{S}$ is a square matrix of order two. If the robot were fully constrained or overconstrained, because actuated, for example, by three or four cables, such a matrix would be rectangular, and there would not exist a unique solution to the problem of determining the set of cable tensions exerting a desires force on the end effector. As discussed earlier, the problem of choosing the best set of cable tensions would become an important issue.

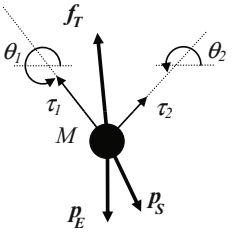

Figure 2 Free body diagram of the end effector

Equation (1) can also be rewritten in this form $\boldsymbol{S\tau} = \boldsymbol{f_T} = -(\boldsymbol{p_S} + \boldsymbol{p_E})$ which is represented graphically in Figure 3. It is apparent that a pose belongs to the SEW only if vector $\boldsymbol{f_T}$ (which is the sum of the cable forces τ_1 and τ_2, and is opposite to the sum of $\boldsymbol{p_S}$ and $\boldsymbol{p_E}$) belongs to the region delimited by the two cables and filled in light gray in Figure 3. For the determination of the SEW, it is therefore necessary to combine the static equilibrium equation with kinematics: the region to which vector $\boldsymbol{f_T}$ must belong is indeed univocally defined once the cable angles θ_i

$(i = 1, 2)$ are known. Such angles depend on the Cartesian position $\{x, y\}$ of the end effector TCP through the equation $\theta_i = \arctan_2((y - A_{iy}), (x - A_{ix}))$, where A_{ix} and A_{iy} $(i = 1, 2)$ are the Cartesian coordinates of the two attachment points (see Figure 1).

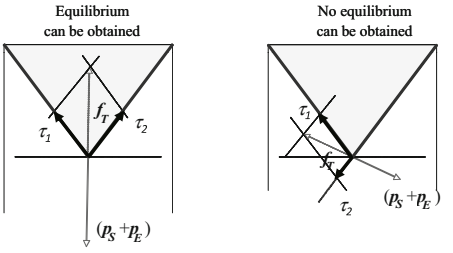

Figure 3 Graphical representations of examples of equilibrium and non-equilibrium conditions

In the absence of the serial linkage the determination of the SEW would by straightforward: only the vertical $\boldsymbol{p_E}$ weight force would be applied to the end effector and the SEW would coincide with the rectangular base polygon whose upper vertices are A_1 and A_2. The presence of the serial linkage, instead, considerably affects the SEW, since it introduces an external force $\boldsymbol{p_S}$ on the end effector whose direction is usually far from being vertical. Figure 4 shows the direction taken by $\boldsymbol{p_S}$ in the base polygon.

It can be noticed that the horizontal component of $\boldsymbol{p_S}$ is often predominant. Hence the presence of $\boldsymbol{p_S}$ makes obtaining static equilibrium while maintaining tension in all cables considerably more difficult. Generally speaking, the heavier the overall mass M of the payload and the end effector, the wider the SEW. This can be appreciated through the subplots in Figure 5 which show how the SEW changes by varying M. In the figures, as an example, M is increased from 2kg (i.e., the value adopted in the prototype discussed in [41]) up to 10kg.

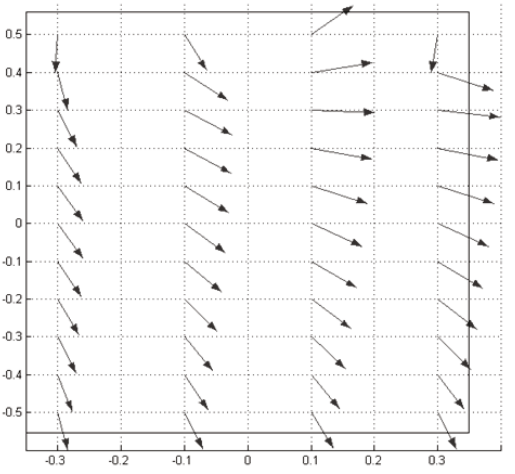

Figure 4 Direction of vector $\boldsymbol{p_S}$ within the robot base polygon (all dimensions in meters)

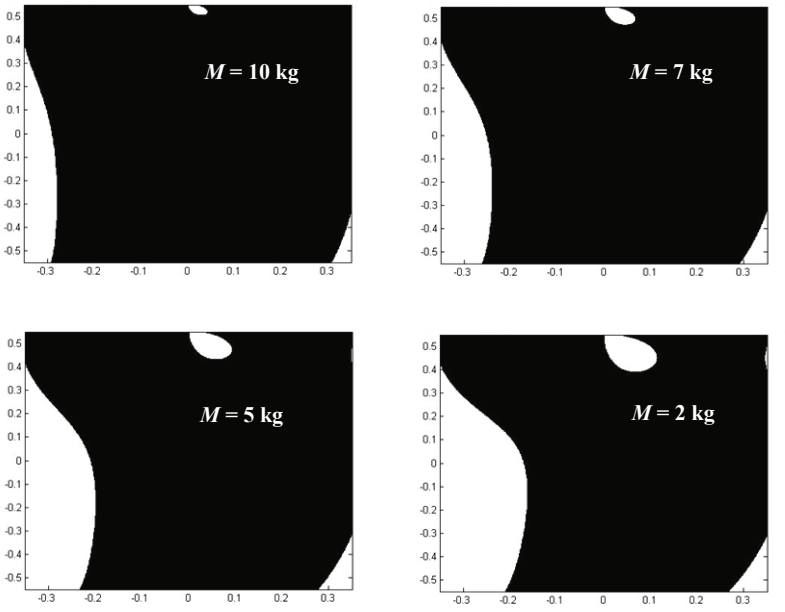

Figure 5 Dependence of the SEW on the mass M (all dimensions in meters)

By observing these figures it would appear preferable increasing considerably the mass M of the payload and the end effector in order to extend the SEW and minimize the impact of the serial linkage. Unfortunately, however, the heavier the mass at the end effector the higher the forces in the cables, and hence the toques that need to be exerted by the motors to obtain static equilibrium. The two subplots in Figure 6 clarify this point: they show the contour-plots (isolines) of the cable forces that are needed to obtain equilibrium when M is 2kg. Both positive and negative forces have been represented. Obviously, when the forces are negative it is not possible to maintain tension in the cables and hence no equilibrium is, in practice, possible. If one recalls the direction of vector $\boldsymbol{p_S}$, shown in Figure 4, it is not surprising that negative forces mainly arise in the cable on the right.

Another important feature to be observed is that at the top of the workspace the cable forces increase very swiftly. Here, for clarity, the force isolines up to 300N have been plotted. Clearly if, for instance, the maximum permissible cable tension was 200N, trying to reach those positions, even in quasi-static conditions, would imply breaking the cables or overcoming the maximum motor torques.

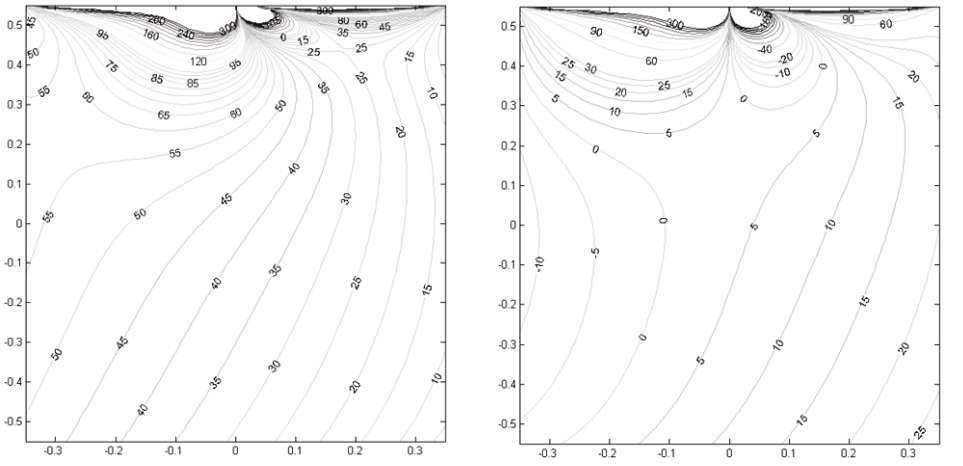

Figure 6 Static cable forces in cable 1, on the left, and cable 2, on the right (axis dimensions in meters, forces in N)

As previously mentioned, the concept of statically feasible workspace allows accounting for both the positivity and boundedness constraints on cable tensions. As an example, Figure 7 shows in gray the SFW of the studied robot having set a 200N maximum force in the cables and a 2kg payload mass M. In the figure, a schematic representation of the robot is overlapped to the SFW to clarify its meaning.

Indeed, only the set of poses belonging to the SFW are poses from which a rest-to-rest motion of the end effector can either start or end. Hence, identifying the SFW is an essential preliminary activity to motion planning. In the following, the planning of dynamically feasible trajectories between two points belonging to the SFW is addressed.

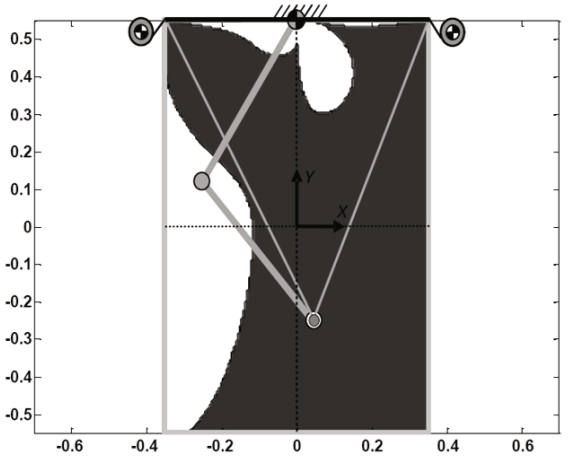

Figure 7 The SFW of the hybrid multi-body cable robot (all dimensions in meters)

4 Parametric Expression of Cable Tensions Along a Generic Path

Let us deduce the parametric expression of the cable tensions for the studied hybrid multi-body cable robot, here employed as an example of generic underconstrained, fully actuated, translational and planar cable robot moving on a vertical plane. The equations reported in this section originate from the ones presented in [39]. However, here the notation has been slightly modified to improve the clarity and prevent confusion with the symbols adopted in the new parametric formulation.

Once a world coordinate frame has been defined, the two dynamic equilibrium equations for the end effector may be stacked in the following matrix form:

$$\boldsymbol{p_E} + \boldsymbol{f_S} + \boldsymbol{f_T} = \boldsymbol{M}\ddot{\boldsymbol{x}}, \tag{2}$$

where the meaning of $\boldsymbol{p_E}$ and $\boldsymbol{f_T}$ has already been clarified above, after Equation (1), and:

- $\boldsymbol{f_S}$ is the force exerted by the passive linkage on the end effector (also including the static component $\boldsymbol{p_S}$).
- $\boldsymbol{M}$ is the Cartesian mass matrix of the end effector.
- $\ddot{\boldsymbol{x}}$ is the Cartesian acceleration vector of the end effector TCP.

By replacing vector $\boldsymbol{f_T}$ with the expression involving the square pseudostatic Jacobian $\boldsymbol{J}$ and the vector of the motor torques $\boldsymbol{\tau}$, Equation (2) can hence be rearranged as follows:

$$\boldsymbol{p_E} + \boldsymbol{f_S} + \boldsymbol{S\tau} = \boldsymbol{M}\ddot{\boldsymbol{x}}. \tag{3}$$

In [39] it has been proved that when a two-link serial support is employed, it exerts a reaction force $\boldsymbol{f_S}$ which takes the following form:

$$\boldsymbol{f_S} = \boldsymbol{I_S}\ddot{\boldsymbol{x}} + \boldsymbol{N_S}(\boldsymbol{J_S^{-1}}\dot{\boldsymbol{x}})^{\boldsymbol{2}} + \boldsymbol{p_S}, \tag{4}$$

where the meaning of vector $\boldsymbol{p_S}$ has already been clarified above, after Equation (1), and:

- $\dot{\boldsymbol{x}}$ and $\ddot{\boldsymbol{x}}$ are the end effector TCP Cartesian velocities and accelerations.
- The elements of the matrices $\boldsymbol{I_S}$ and $\boldsymbol{N_S}$ depend on the inertial and geometrical properties of the serial linkage and the positions of its links (and hence, in the end, on the Cartesian position $\boldsymbol{x}$ of the end effector TCP).
- The elements of matrix $\boldsymbol{J_S}$ only depend on the lengths and the positions of the links.

The following general expression for the tension vector $\boldsymbol{\tau}$ can hence be written:

$$\boldsymbol{\tau} = \boldsymbol{S^{-1}}\left[(\boldsymbol{M} - \boldsymbol{I_S})\ddot{\boldsymbol{x}} - \boldsymbol{N_S}(\boldsymbol{J_S^{-1}}\dot{\boldsymbol{x}})^{\boldsymbol{2}} - (\boldsymbol{p_S} + \boldsymbol{p_E})\right]. \tag{5}$$

A more compact expression for $\boldsymbol{\tau}$ can be obtained by setting $\boldsymbol{B} = \boldsymbol{S^{-1}}(\boldsymbol{M} - \boldsymbol{I_S})$, $\boldsymbol{C} = \boldsymbol{S^{-1}}\boldsymbol{N_S}$, and $\boldsymbol{d} = -\boldsymbol{S^{-1}}(\boldsymbol{p_S} + \boldsymbol{p_E})$:

$$\boldsymbol{\tau} = \boldsymbol{B}\ddot{\boldsymbol{x}} - \boldsymbol{C}(\boldsymbol{J_S^{-1}}\dot{\boldsymbol{x}})^{\boldsymbol{2}} + \boldsymbol{d}. \tag{6}$$

Now, let us introduce the path parameter l, i.e., a scalar parameter used to specify the geometric path to be followed by the TCP: $\boldsymbol{x} = \boldsymbol{x}(l)$. l can also be interpreted as the position variable, i.e., the coordinate specifying the TCP position along the path. The following are the expressions of $\dot{\boldsymbol{x}}$ and $\ddot{\boldsymbol{x}}$ as functions of l:

$$\dot{\boldsymbol{x}} = \dot{l}\boldsymbol{x'}, \qquad \ddot{\boldsymbol{x}} = \ddot{l}\boldsymbol{x'} + \dot{l}^2\boldsymbol{x''}. \tag{7}$$

In Equation (7), as usual, overdots denote time derivatives and primes denote derivatives with respect to the path parameter; additionally, the explicit dependence of $\boldsymbol{x'}$ and $\boldsymbol{x''}$ on l has been omitted. The first ($\dot{l}$) and second ($\ddot{l}$) time derivatives of the path parameter l along the path are sometimes called respectively the pseudo-velocity and the pseudo-acceleration of the path. By introducing these expression in Equation (6), we are finally given the cable tensions in parametric form:

$$\boldsymbol{\tau} = \boldsymbol{B}\boldsymbol{x'}\ddot{l} - [\boldsymbol{C}(\boldsymbol{J_S^{-1}}\boldsymbol{x'})^{\boldsymbol{2}} - \boldsymbol{B}\boldsymbol{x''}]\dot{l}^2 + \boldsymbol{d} := \boldsymbol{p}\ddot{l} - \boldsymbol{q}\dot{l}^2 + \boldsymbol{d} \tag{8}$$

with the obvious meaning for $\boldsymbol{p}$ and $\boldsymbol{q}$.

A cable tension vector $\boldsymbol{\tau}$ is feasible when all its components are constrained between minimum and maximum tension values. In cable robots such a condition must hold both at rest and during motion.

5 Constraints on the First and Second Derivatives of the Path Parameter

Once the parametric expression of the cable tension vector is available, it is possible to impose the constraints which allow avoiding cable slackness ($\boldsymbol{\tau} \succ \boldsymbol{0}$) and excessive tensioning ($\boldsymbol{\tau} \prec \boldsymbol{\tau_{\max}}$). The following bilateral inequality holds:

$$\boldsymbol{0} \prec \boldsymbol{p}\ddot{l} - \boldsymbol{q}\dot{l}^2 + \boldsymbol{d} \prec \boldsymbol{\tau}_{\max}. \tag{9}$$

The symbol $\prec$ stands for the componentwise inequality. It should be noted that $\boldsymbol{\tau}_{\max}$ is the vector of the maximum permissible tensions, related to the torque limits of the actuators or to tensile force limits of the cables, while, referring to the lower bound, a minimum allowed tension could replace to the null value for safer operation. Here, however, without lack of generality, the null value is considered. It is also worth observing that:

- $\boldsymbol{d}$ only depends on the end effector TCP position in the planar workspace($\boldsymbol{x}$).
- $\boldsymbol{p}$ depends on both $\boldsymbol{x}$ and the first derivative of $\boldsymbol{x}$ with respect to the path parameter l (i.e., $\boldsymbol{x'}$).
- $\boldsymbol{q}$ depends on $\boldsymbol{x}$, and on both the first and second derivatives of $\boldsymbol{x}$ with respect to l (i.e., $\boldsymbol{x'}$ and $\boldsymbol{x''}$).

Equation (9) may be also written in the following form, referred to the i^{th} cable:

$$0 < \tau_i := p_i\ddot{l} - q_i\dot{l}^2 + d_i < \tau_{i_{\max}}. \tag{10}$$

Remark 5.1 Each element d_i of $\boldsymbol{d}$ corresponds to the i^{th} cable tension in static conditions (see Equation (10)). Hence, $d_i > 0$ in the SFW.

The inequalities in Equation (10) hold for any path and trajectory, and explicitly relate the pseudo-velocity $\dot{l}$ and the pseudo-acceleration $\ddot{l}$ along the path. They can therefore be employed to translate the physical constraints on the cable tensions into limits on the velocity and acceleration of the end effector TCP along the path. To this purpose, it is convenient to rewrite the inequalities in Equation (10) as follows:

$$p_i \ddot{l} > u_i := q_i \dot{l}^2 - d_i, \quad i = 1, 2, \tag{11}$$

$$p_i \ddot{l} < s_i := q_i \dot{l}^2 - d_i + \tau_{i_{\max}}, \quad i = 1, 2, \tag{12}$$

where the two new functions u_i and s_i have been defined.

Lemma 5.2 *At any point of the SFW:*

$$\exists \dot{l}_{\lim} > 0 | \forall 0 < |\dot{l}| \leq \dot{l}_{\lim} \Rightarrow u_i < 0, \quad s_i > 0, \quad i = 1, 2.$$

Proof Let i be either 1 or 2. Assume $q_i \leq 0$. Since $d_i > 0$ (see Remark 5.1), Equation (11) shows that $u_i < 0$ for any $\dot{l}$. Let then define $\dot{l}_{u_i \ \lim} = \dot{l}_{\max_i} = +\infty$. As far as s_i is concerned, since $-d_i + \tau_{i_{\max}} > 0$ (otherwise cable tensions would equal or overcome the maximum permissible values in static conditions, which cannot happen in the SFW), Equation (12) shows that it is possible to reduce $\dot{l}$ until $s_i > 0$. As a matter of fact, $\exists \dot{l}_{s_i \ \lim} > 0 | q_i \dot{l}^2_{s_i \ \lim} > d_i - \tau_{i_{\max}}$, hence, $\forall \dot{l} | 0 < |\dot{l}| \leq \dot{l}_{s_i \ \lim} \Rightarrow s_i > 0$.

Now assume the opposite: $q_i > 0$. Equation (12) proves that $s_i > 0$ for any $\dot{l}$. As done before, let us define $\dot{l}_{s_i \ \lim} = \dot{l}_{\max_i} = +\infty$. Equation (11) shows that a suitably low value of $\dot{l}$ can ensure $u_i < 0$. In symbols, $\exists \dot{l}_{u_i \ \lim} > 0 | q_i \dot{l}^2_{u_i \ \lim} < d_i$, and consequently, $\forall \dot{l} | 0 < |\dot{l}| \leq \dot{l}_{u_i \ \lim} \Rightarrow u_i < 0$.

The four values $\dot{l}_{u_i \ \lim}$ $(i = 1, 2)$ and $\dot{l}_{s_i \ \lim}$ $(i = 1, 2)$ are usually different, however, by defining the limit velocity $\dot{l}_{\lim} = \min(\dot{l}_{u_1 \ \lim}, \dot{l}_{s_1 \ \lim}, \dot{l}_{u_2 \ \lim}, \dot{l}_{s_2 \ \lim})$ one proves the lemma. ∎

In practice, $\dot{l}_{\max_i}$ cannot be set equal to $+\infty$ but it is a velocity constraint which should be related to the i^{th} actuator performances[50], or to more conservative and safe design specifications. In general, such values are however much higher than $\dot{l}_{u_i \ \lim}$ and $\dot{l}_{s_i \ \lim}$, whose maximum values are respectively $\sqrt{\frac{d_i}{q_i}}$ and $\sqrt{\frac{d_i - \tau_{i_{\max}}}{q_i}}$.

Theorem 5.3 *As long as the absolute value of the pseudo-velocity is less than, or equal to, $\dot{l}_{\lim}$, at any point of the SFW the bilateral bounds on cable tensions can be translated into bilateral bounds on the pseudo-acceleration along the prescribed path. At any point of the SFW the upper bound of the acceleration is positive and the lower bound is negative:*

$$\forall \dot{l} | 0 < |\dot{l}| \leq \dot{l}_{\lim} : \exists \ddot{l}_{lb} < 0, \ddot{l}_{ub} > 0 | \ddot{l}_{lb} < \ddot{l} < \ddot{l}_{ub} \Rightarrow 0 < \tau_i < \tau_{i_{\max}}, \quad i = 1, 2.$$

Proof Let i be either 1 or 2. Assume $p_i \leq 0$. By applying Lemma 5.2 twice, Equations (11) and (12) provide respectively a possible positive upper bound $\ddot{l}_{i_{ub}} = \frac{u_i}{p_i} > 0$ and a possible negative lower bound $\ddot{l}_{i_{lb}} = \frac{s_i}{p_i} < 0$ for the pseudo-acceleration $\ddot{l}$ along the path. Positive or negative infinity solutions are theoretically acceptable.

Now assume $p_i > 0$. Through the same reasoning it is proved that $\frac{u_i}{p_i} < 0$ becomes a possible negative lower bound $\ddot{l}_{i_{lb}}$ for $\ddot{l}$, while $\frac{s_i}{p_i} > 0$ becomes a possible positive upper bound $\ddot{l}_{i_{ub}}$.

Then, by taking the most restrictive interval defined through the four bounds $\ddot{l}_{i_{ub}}$ $(i = 1, 2)$ and $\ddot{l}_{i_{lb}}$ $(i = 1, 2)$, i.e., by defining $\ddot{l}_{ub} = \min\left(\ddot{l}_{1_{ub}}, \ddot{l}_{2_{ub}}\right)$ and $\ddot{l}_{lb} = \max\left(\ddot{l}_{1_{lb}}, \ddot{l}_{2_{lb}}\right)$ one obtains the pseudo-acceleration interval $]\ddot{l}_{lb}, \ddot{l}_{ub}[$ ensuring $0 < \tau_i < \tau_{i_{\max}}$. This proves the theorem. ∎

In summary, at any point of the SFW, once an upper bound $\dot{l}_{\lim}$ ensuring both negative u_i functions and positive s_i functions has been determined for the end effector pseudo-velocity $\dot{l}$, there always exist a positive upper bound $\ddot{l}_{ub}$ and a negative lower bound $\ddot{l}_{lb}$ for the pseudo-acceleration $\ddot{l}$, guaranteeing that, as long as $0 < |\dot{l}| \leq \dot{l}_{\lim}$ and $\ddot{l}_{lb} < \ddot{l} < \ddot{l}_{ub}$, each cable tension τ_i is simultaneously positive and below the maximum permissible value, i.e., $0 < \tau_i < \tau_{i_{\max}}$ $(i = 1, 2)$. In general, these bounds are not constant but vary along the path, so they should be computed as functions of a path coordinate l by adopting a suitable discretization of the path itself. The fact that $\ddot{l}_{lb} < 0$ and $\ddot{l}_{ub} > 0$ simplifies the planning of the trajectory because it allows increasing, reducing or keeping constant the velocity at any point.

6 Theory Application

The theoretical achievements discussed above represent a generalization of the method presented in [39] and experimentally validated in [41], which was originally confined to straight line and circular paths. The numerical results presented in [39] and the experimental proofs discussed in [41] can therefore be considered an adequate validation of this theory: the same results can be obtained by applying this more general approach to the test cases discussed in such papers.

Generally speaking, any trajectory planning method yielding a trajectory in time $l(t)$ meeting the pseudo-velocity and pseudo-acceleration bounds computed above can assure that cable tensions are always positive and below the maximum permissible values along the path. The solution of this problem goes beyond the scope of this paper but, just with the aim of providing a representative example, the case of $l(t)$ expressed through a quintic polynomial is discussed here. Such an expression is particularly suitable to point-to-point planning and leads to trajectories that can be made smooth enough not to excite the vibrational phenomena induced by cable elasticity. Additionally, minimum travel time can be easily computed. Hence, let us express the path coordinate l through the following polynomial: $l(t) = b_0 + b_1 t + b_2 t^2 + b_3 t^3 + b_4 t^4 + b_5 t^5$, where $0 \leq l \leq L_t$ and L_t is the path length. Let 0 and t_f be respectively the initial and final trajectory time and let us impose zero velocity and acceleration at 0 and t_f. It can be verified that the coefficients satisfying such boundary conditions are: $b_0 = 0$, $b_1 = 0$, $b_2 = 0$, $b_3 = \frac{10L_t}{t_f^3}$, $b_4 = \frac{-15L_t}{t_f^4}$, and $b_5 = \frac{6L_t}{t_f^5}$. The resulting trajectory is symmetric with respect to the mean time $t_m = \frac{t_f}{2}$: at $t = t_m$ the maximum velocity $\dot{l}_{\max} = \frac{15L_t}{8t_f}$ is achieved and the acceleration is zero. In the first half of the trajectory the acceleration is always positive while in the second half the acceleration is always negative. The maximum acceleration and deceleration values are identical in absolute value: $\ddot{l}_{\max} = \frac{10L_t}{t_f^2\sqrt{3}}$. Hence, in order to meet

both the velocity and the acceleration constraints, t_f should be chosen so that $\dot{l}_{\max} \leq \dot{l}_{\lim}$ and $\ddot{l}_{\max} \leq \min\left(\min\left(\ddot{l}_{ub}|_0^{\frac{L_t}{2}}\right), \left|\max\left(\ddot{l}_{lb}|_{\frac{L_t}{2}}^{L_t}\right)\right|\right)$. The minimum travel time t_f can hence be computed as follows: $\max\left(\sqrt{\frac{10L_t}{\ddot{l}_{\max}\sqrt{3}}}, \frac{15L_t}{8\dot{l}_{\max}}\right)$.

For continuous trajectory planning the method proposed in [51] (which makes use of a concatenation of fifth-order polynomials) might be extended to cope with not only constant but path-dependent velocity and acceleration limits. Before planning the trajectory, it is therefore crucial to choose an appropriate value of the limit velocity $\dot{l}_{lim}$. Such a choice affects both the size of the subset of the SFW where it is possible to move (i.e., where there exist $\ddot{l}_{ub}$ and $\ddot{l}_{lb}$), and the values of the acceleration bounds, which, in turn, affect the travel time. As proved in Lemma 5.2, $\dot{l}_{lim}$ must be chosen so that negative u_i and positive s_i functions are obtained in the whole subset of the SFW where the end effector of the robot needs to be moved. As an example, Figure 8 shows the contour plots of the limit velocity values ensuring $u_i < 0$ in the studied robot for any straight line path (i.e., a path with constant $\boldsymbol{x'}$ and $\boldsymbol{x''} = \mathbf{0}$). At each position the value plotted represents the most stringent constraint obtained by varying the path direction $\boldsymbol{x'}$ while keeping $\boldsymbol{x''} = \mathbf{0}$. A similar plot could be obtained also for the s_i functions, however, ensuring negative u_i functions introduces more stringent constraints on the velocity, and so the plot referring to s_i functions is omitted for brevity. In Figure 8 it is also highlighted that in all the gray area negative u_i functions cannot be assured if the limit velocity is set, for example, equal to or higher than 1.5m/s. The gray area creates a discontinuity between regions where negative u_i functions are assured. A different choice of $\dot{l}_{\lim}$ could either enlarge or decrease the wideness of such a discontinuity and hence would allow coping with it if necessary. It is however interesting to observe that what happens in such a gray region is that it is not possible to get, concurrently, negative lower bounds and positive upper bounds for the acceleration. It could happen, however, that in order to get positive and bounded tensions both the acceleration limits should be either positive or negative. Which does not imply, in general, that it is impossible to cross the gray region while moving in a straight line from a start point to an end point both belonging to the SFW. Of course the planning of feasible trajectories in such a case becomes more difficult, and will be a matter of future investigation.

Whichever is the limit velocity $\dot{l}_{\lim}$ chosen, it follows from Theorem 5.3 that it is possible to compute the acceleration bounds. As a representative example Figure 9 shows the worst case acceleration bounds with $\dot{l}_{\lim} = 1.5$m/s for a generic straight line path, i.e., the lowest upper bounds and the highest lower bounds that can be computed at any position of the workspace by varying the path direction ($\boldsymbol{x'}$). This plot gives a visual representation of the areas where performing feasible trajectories is undemanding. Indeed, this is just a global evaluation, an effective planning instead imposes computing the exact bounds for the specific path. Examples can be found in [39] and [41].

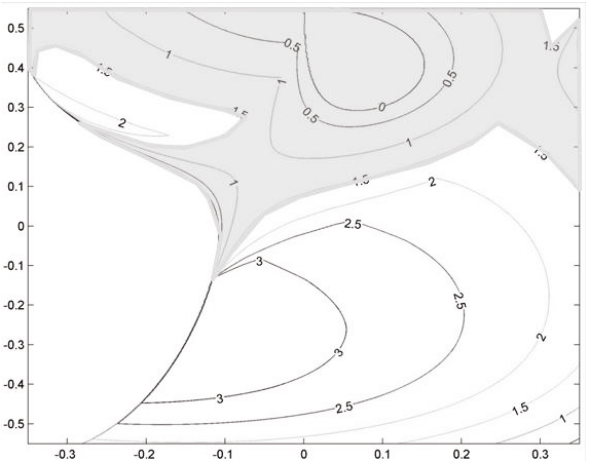

Figure 8 $\dot{l}_{\lim}$ values assuring $u_i < 0$ (axis dimensions in meters, velocity values in m/s)

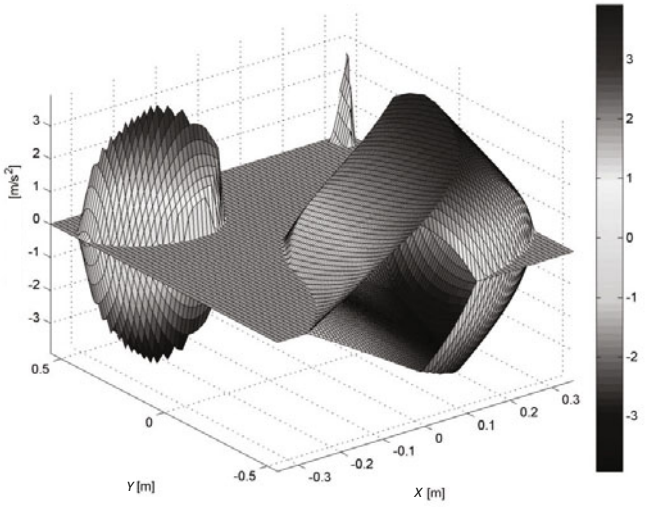

Figure 9 Strictest acceleration range for a straight line path with $\dot{l}_{\lim} = 1.5$m/s

At first glance, on the basis of what has been presented above, low $\dot{l}_{\lim}$ values appear preferable: not only do they extend the SFW subset where it is possible to concurrently accelerate and decelerate, but also they lead to wider bounds on $\ddot{l}$ (see the acceleration bound expressions in the proof of Theorem 5.3). It is however apparent that low $\dot{l}_{\lim}$ values may lead to overconservative trajectory planning and poor travel time. A suitable tradeoff should therefore be sought. Different strategies for choosing $\dot{l}_{\lim}$ might be proposed: at a minimum, either a single value holding for the whole SFW subset of interest or different "path selective" values might be adopted.

7 Conclusions

Cable robots have a great potential and promise to significantly increase performances in terms of payload, workspace and dynamics compared to serial industrial robots. It has been observed that underconstrained and planar cable robots can find application in several fields and in particular in the fast moving consumer goods industry. The hybrid multi-body cable robot topology discussed in this paper belongs to the family of underconstrained and planar cable robots and allows combining some important advantages of traditional and cable manipulators, but, at the same time, worsen the problem of proper cable tensioning both in static and dynamic conditions. This problem has been tackled by developing an approach ensuring dynamically feasible trajectories within the statically feasible workspace (SFW), whose definition has also been introduced in the paper. The SFW definition accounts for the positivity and boundedness constraints on the cable tensions in the presence of just the gravity wrench. The approach proposed to plan dynamically feasible trajectories is based on translating cable tension bilateral bounds into limits on the velocity and acceleration of the end effector along the path, which is assumed to be known. A general and novel formulation of the approach has been proposed in this paper, which is based on a parametric formulation of the cable tensions along a generic path. It has been proved that as long as the pseudo-velocity of the end effector is below a limit depending on some functions named u_i and s_i, and the pseudo-acceleration is within a range identified through the dynamic model, proper cable tensioning is assured. It has also been proved that the limit velocity always exists in the SFW and that the lower bounds of the acceleration range are always negative while the upper bounds are always positive. These kinematic limits can then be incorporated into any trajectory planning algorithm.

It is important to underline that the method developed is not a trajectory verifier, but a method to a-priori satisfy cable tension constraints. In other words, the method a-priori ensures that cable tensions neither drop to zero nor exceed the maximum permissible tension during the motion, provided that an effective motion controller allows tracking the planned trajectory with negligible errors. What is more important the low computational complexity of this method makes it suitable for implementation in real time systems. Which paves the way for industrial use.

References

[1] Albus J, Bostelman R, and Dagalakis N, The NIST robocrane, *Journal of Robotic Systems*, 1993, **10**(5): 709–724.

[2] Ming A and Higuchi T, Study on multiple degree-of-freedom positioning mechanism using wires (part 1) - concept, design and control, *International Journal of Japan Social Engineering*, 1994, **28**(2): 131–138.

[3] Higuchi T, Ming A, and Jiang Y J, Application of multi-dimensional wire cranes in construction,

Proceedings of the 5*th International Symposium on Robotics in Construction* (*ISRC*'88), Tokyo, Japan, 1988.

[4] Holland C S and Cannon D J, Cable array robot for material handling, *United States Patent*, US 6'826'452 B1, 2004.

[5] Oh S R, Ryu J C, and Agrawal S K, Dynamics and control of a helicopter carrying a payload using a cable-suspended robot, *ASME Journal of Mechanical Design*, 2006, **128**(5): 1113–1121.

[6] Maeda K, Tadokoro S, Takamori T, Hiller M, and Verhoeven R, On design of a redundant wire-driven parallel robot WARP manipulator, *Proceedings of the* 1999 *IEEE International Conference on Robotics and Automation* (*ICRA*'99), Detroit, MI, USA, 1999.

[7] Kawamura S, Kino H, and Won C, High-speed manipulation by using parallel wire-driven robots, *Robotica*, 2000, **18**(1): 13–21.

[8] Blair J, NIST robocrane cuts aircraft maintenance costs, 2006 [on line], http://www.nist.gov/el/isd/robo-070606.cfm.

[9] Pott A, Mtherich H, Kraus W, Schmidt V, Miermeister P, and Verl A, IPAnema: A family of cable-driven parallel robots for industrial applications, *Cable-Driven Parallel Robots* (ed. by Bruckmann T and Pott A), Springer-Verlag, Berlin, Heidelberg, 2013, 119–134.

[10] Lafourcade P, Llibre M, and Reboulet C, Design of a parallel wire-driven manipulator for wind tunnels, *Proceedings of the Workshop on Fundamental Issues and Future Research Directions for Parallel Mechanisms and Manipulators*, Quebec City, Quebec, Canada, 2002.

[11] Kawamura S and Ito K, A new type of master robot for teleoperation using a radial wire drive system, *Proceedings of the IEEE/RSJ International Conference on Intelligent Robots and Systems*, Yokohama, Japan, 1993.

[12] Williams R L II, Cable-suspended haptic interface, *International Journal of Virtual Reality*, 1998, **3**(3): 13–21.

[13] Gallina P, Rosati G, and Rossi A, 3-d.o.f. wire driven planar haptic interface, *Journal of Intelligent and Robotic Systems*, 2001, **32**: 23–36.

[14] Williams R L II, Albus J S, and Bostelman R V, 3D cable-based cartesian metrology system, *Journal of Robotic Systems*, 2004, **21**(5): 237–257.

[15] Hamid S and Simaan N, Design and synthesis of wire-actuated universal-joint wrists for surgical applications, *Proceedings of the* 2009 *IEEE International Conference on Robotics and Automation* (*ICRA*'09), Kobe, Japan, 2009.

[16] Rosati G, Gallina P, Rossi A, and Masiero S, Wire-based robots for upper-limb rehabilitation, *International Journal of Assistive Robotics and Mechatronics*, 2006, **7**(2): 3–10.

[17] Ying M and Agrawal S K, Design of a cable-driven arm exoskeleton (CAREX) for neural rehabilitation, *IEEE Transactions on Robotics*, 2012, **28**(4): 922–931.

[18] Nan R, Five hundred meter aperture spherical radio telescope, *Science in China: Series G, Physics, Mechanics & Astronomy*, 2006, **49**(2): 129–148.

[19] Cone L L, Skycam: An aerial robotic camera system, *Byte*, 1985, **1**(10): 122–132.

[20] Spydercam, 2012 [on line] http://www.spydercam.com/.

[21] Tadokoro S, Verhoeven R, Hiller M, and Takamori T, A portable parallel manipulator for search and rescue at large-scale urban earthquakes and an identification algorithm for the installation in unstructured environments, *Proceedings of the* 1999 *IEEE/RSJ International Conference on Intelligent Robots and Systems* (*IROS*'99), Kyongju, Japan, 1999.

[22] Merlet J P, Kinematics of the wire-driven parallel robot MARIONET using linear actuators,

Proceedings of the 2008 *IEEE International Conference on Robotics and Automation* (*ICRA* '08), Pasadena, California, USA, 2008.

[23] Izard J B, Gouttefarde M, Michelin M, Tempier O, and Baradat C, A reconfigurable robot for cable-driven parallel robotic and industrial scenario proofing, *Cable-Driven Parallel Robots* (ed by Bruckmann T and Pott A), Springer-Verlag, Berlin, Heidelberg, 2013: 135–148.

[24] Fattah A and Agrawal S K, On the design of cable-suspended planar parallel robots, *Journal of Mechanical Design*, 2005, **127**: 1021–1028.

[25] Tadokoro S, Murao Y, Hiller M, Murata R, Kohkawa H, and Matsushima T, Motion base with 6-dof by parallel cable drive architecture, *IEEE/ASME Transaction on Mechatronics*, 2002, **7**(2): 115–123.

[26] Williams R L II and Gallina P, Translational planar cable-direct-driven robots, *Journal of Intelligent and Robot Systems*, 2003, **37**: 69–96.

[27] Riechel A T and Ebert-Uphoff I, Force feasible workspace analysis for underconstrained point-mass cable robots, *Proceedings of the* 2004 *IEEE International Conference on Robotics and Automation* (*ICRA* '04), New Orleans, Louisiana, USA, 2004.

[28] Gorman J J, Jablokow K W, and Cannon D J, The cable array robot: Theory and experiment, *Proceedings of the* 2001 *IEEE International Conference on Robotics and Automation* (*ICRA* '01), Seoul, Korea, 2001.

[29] Oh S R and Agrawal S K, Cable-suspended planar parallel robots with redundant cables: Controllers with positive cable tensions, *Proceedings of the* 2003 *IEEE International Conference on Robotics and Automation*, Taipei, 2003.

[30] Carricato M and Abbasnejad G, Direct geometrico-static analysis of under-constrained cable-driven parallel robots with 4 cables, *Cable-Driven Parallel Robots* (ed. by Bruckmann T and Pott A), Springer-Verlag, Berlin, Heidelberg, 2013, 269–285.

[31] Lamaury J and Gouttefarde M, A tension distribution method with improved computational efficiency, *Cable-Driven Parallel Robots* (ed. by Bruckmann T and Pott A), Springer-Verlag, Berlin, Heidelberg, 2013, 269–285.

[32] Campbell P D, Swaim P L, and Thompson C J, Charlotte robot technology for space and terrestrial applications, SAE Article 951520, *Proceedings of the* 25*th International Conference on Environmental Systems*, San Diego, California, 1995.

[33] Castelli G, Ottaviano E, and Gonzlez A, Analysis and simulation of a new cartesian cable-suspended robot, *Proceedings of the Institution of Mechanical Engineers, Part C: Journal of Mechanical Engineering Science*, 2010, **224**(8): 1717–1726.

[34] Zi B, Duan B Y, Du J L, and Bao H, Dynamic modeling and active control of a cable-suspended parallel robot, *Mechatronics*, 2008, **18**(1): 1–12.

[35] Taghavi A, Behzadipour S, Khalilinasab N, and Zohoor H, Workspace improvement of two-link cable-driven mechanisms with spring cable, *Cable-Driven Parallel Robots* (ed. by Bruckmann T and Pott A), Springer-Verlag, Berlin, Heidelberg, 2013, 201–213.

[36] Notash L and Kamalzadeh A, Inverse dynamics of wire-actuated parallel manipulators with a constraining linkage, *Mechanism and Machine Theory*, 2007, **42**(9): 1103–1118.

[37] Kino H and Kawamura S, Development of a serial link structure/parallel wire system for a force display, *Proceedings of the* 2002 *IEEE International Conference on Robotics and Automation* (*ICRA* '02), Washington, D.C., USA, 2002.

[38] Izard J B, Gouttefarde M, Baradat C, Culla D, and Sall D, Integration of a parallel cable-driven

robot on an existing building faade, *Cable-Driven Parallel Robots* (ed by Bruckmann T and Pott A), 149–164, Springer-Verlag, Berlin, Heidelberg, 2013.

[39] Trevisani A, Underconstrained planar cable-direct-driven robots: A trajectory planning method ensuring positive and bounded cable tensions, *Mechatronics*, 2010, **20**: 113–127.

[40] Trevisani A, Gallina P, and Williams R L II, Cable-direct-driven robot (CDDR) with passive SCARA support: Theory and simulation, *Journal of Intelligent and Robotic Systems*, 2006, **46**: 73–94.

[41] Trevisani A, Experimental validation of a trajectory planning approach avoiding cable slackness and excessive tension in underconstrained translational planar cable-driven robots, *Cable-Driven Parallel Robots* (ed by Bruckmann T and Pott A), Springer-Verlag, Berlin, Heidelberg, 2013, 23–29.

[42] Alp A B and Agrawal S K, Generation of feasible set points and control of a cable robot, *IEEE Transactions on Robotics*, 2006, **22**: 551–558.

[43] Behzadipour S and Khajepour A, Time-optimal trajectory planning in cable-based manipulators, *IEEE Transactions on Robotics*, 2006, **22**: 559–563.

[44] Barrette G and Gosselin C M, Determination of the dynamic workspace of cable-driven planar parallel mechanisms, *ASME Journal of Mechanical Design*, 2005, **127**(2): 242–248.

[45] Gouttefarde M and Gosselin C M, Analysis of the wrench-closure-workspace of planar parallel cable-driven mechanisms, *IEEE Transactions on Robotics*, 2006, **22**: 434–445.

[46] Bosscher P, Riechel A T, and Ebert-Uphoff I, Wrench-feasible workspace generation for cable-driven robots, *IEEE Transactions on Robotics*, 2006, **22**: 890–902.

[47] Pham C B, Yeo S H, Yang G, Kurbanhusen M S, and Chen I M, Force-closure workspace analysis of cable-driven parallel mechanisms, *Mechanism and Machine Theory*, 2006, **41**: 53–69.

[48] Gosselin C M, Global planning of dynamically feasible trajectories for three-dof spatial cable-suspended parallel robots, *Cable-Driven Parallel Robots* (ed by Bruckmann T and Pott A), Springer-Verlag, Berlin, Heidelberg, 2013, 3–22.

[49] Oh S R and Agrawal S K, Generation of feasible set points and control of a cable robot, *IEEE Transactions on Robotics*, 2006, **22**(3): 551–558.

[50] Bobrow J E, Dubowsky S, and Gibson J S, Time-optimal control of robotic manipulators along specified paths, *International Journal of Robotics Research*, 1985, **4**(3): 3–17.

[51] Macfarlane S and Croft E A, Jerk-bounded manipulator trajectory planning: Design for real-time applications, *IEEE Transactions on Robotic Automation*, 2003, **19**(1): 42–52.